

This article was downloaded by:[MPI Max-Planck-Institute Fuer Quantenoptik]  
On: 9 August 2007  
Access Details: [subscription number 779599386]  
Publisher: Taylor & Francis  
Informa Ltd Registered in England and Wales Registered Number: 1072954  
Registered office: Mortimer House, 37-41 Mortimer Street, London W1T 3JH, UK



## Journal of Modern Optics

Publication details, including instructions for authors and subscription information:  
<http://www.informaworld.com/smpp/title~content=t713191304>

### Short XUV pulses to characterize field-free molecular alignment

Online Publication Date: 01 May 2007

To cite this Article: LéPine, F., Kling, M. F., Ni, Y. F., Khan, J., Ghafur, O., Martchenko, T., Gustafsson, E., Johnsson, P., Varjú, K., Remetter, T., L'huillier, T. and Vrakking, M. J. J. (2007) 'Short XUV pulses to characterize field-free molecular alignment', Journal of Modern Optics, 54:7, 953 - 966

To link to this article: DOI: 10.1080/09500340601022490

URL: <http://dx.doi.org/10.1080/09500340601022490>

PLEASE SCROLL DOWN FOR ARTICLE

Full terms and conditions of use: <http://www.informaworld.com/terms-and-conditions-of-access.pdf>

This article maybe used for research, teaching and private study purposes. Any substantial or systematic reproduction, re-distribution, re-selling, loan or sub-licensing, systematic supply or distribution in any form to anyone is expressly forbidden.

The publisher does not give any warranty express or implied or make any representation that the contents will be complete or accurate or up to date. The accuracy of any instructions, formulae and drug doses should be independently verified with primary sources. The publisher shall not be liable for any loss, actions, claims, proceedings, demand or costs or damages whatsoever or howsoever caused arising directly or indirectly in connection with or arising out of the use of this material.

© Taylor and Francis 2007

## Short XUV pulses to characterize field-free molecular alignment

F. LÉPINE\*<sup>†</sup>, M. F. KLING<sup>†</sup>, Y. F. NI<sup>†</sup>, J. KHAN<sup>†</sup>, O. GHAFUR<sup>†</sup>,  
T. MARTCHENKO<sup>†</sup>, E. GUSTAFSSON<sup>‡</sup>, P. JOHNSON<sup>‡</sup>, K. VARJU<sup>‡</sup>,  
T. REMETTER<sup>‡</sup>, A. L'HUILLIER<sup>‡</sup> and M. J. J. VRAKKING<sup>†</sup>

<sup>†</sup>FOM-Institute AMOLF, Kruislaan 407, 1098 SJ Amsterdam,  
The Netherlands

<sup>‡</sup>Department of Physics, Lund University, PO Box 118,  
SE-221 00 Lund, Sweden

(Received 31 July 2006)

We present experiments on field-free molecular alignment of N<sub>2</sub> and CO<sub>2</sub> probed with short XUV pulses that are obtained via high-harmonic generation. The XUV pulses induce a dissociative ionization or a Coulomb explosion of the molecule, where the fragment ion recoil (measured using the velocity map imaging technique) provides information on the alignment of the parent molecule at the time of ionization. We discuss how photoelectron detection may in future allow the determination of molecular-frame photoelectron angular distributions and molecular structure.

### 1. Introduction

When molecules are placed at the focus of an intense linearly polarized laser field, they align their internuclear axis to the direction of the polarization of the laser. This dynamic alignment is a consequence of the fact that the energy of the dipole induced by the laser by means of the molecular anisotropic polarizability is minimized when the molecule is aligned [1]. Dynamic alignment has attracted a lot of attention in recent years, and is one of the prime examples of a new field of ‘molecular optics’ that is emerging, where intense lasers are used to control both the internal and external degrees of freedom of atoms and molecules [2]. Much of the early work on dynamic alignment concentrated on alignment of molecules with the strong laser field present [3]. However, the laser can also excite a rotational wavepacket by impulsive stimulated Raman scattering that leads to an alignment of the molecule (or even, under suitable experimental conditions, orientation) after the laser pulse is gone [4, 5]. The first demonstration of *field-free* alignment was obtained in pump–probe experiments where iodine molecules were excited with an intense infrared alignment pulse and where the alignment was monitored by Coulomb explosion imaging at a variable delay, using a second infrared laser that fragmented the

---

\*Corresponding author. Email: lepine@lasim.univ-lyon1.fr

molecules into charged atomic fragments [6], whose recoil velocity was measured by means of an imaging detector [7]. At well-defined time delays given by the rotational period of the molecule, alignment revivals occurred where the angular width suddenly increased or decreased during several picoseconds. Other researchers have significantly extended this work. Optimization of field-free alignment under the influence of a sequence of pulses has been studied [8], as well as the use of elliptically polarized laser beams in order to achieve field-free 3D alignment [9]. Interest in the generation of field-free aligned molecules is motivated by the fact that there are many applications in physics (optical pulse compression [10], high harmonic generation [11]) and chemistry (stereochemistry of bi-molecular reactions, photodissociation and photoionization [12, 13]) where field-free aligned molecules may be used advantageously. Beautiful recent examples have been the use of samples of field-free aligned molecules in high harmonic generation experiments aimed at determining the electronic [14] and nuclear [15] structure of molecules. While the term 'field-free molecular alignment' is commonly reserved for experiments where the anisotropy in the molecular angular distribution is explicitly measured or used, both the excitation of a coherent superposition of rotational eigenstates using a short pump laser pulse and the detection of revival structures using a time-delayed probe laser pulse precede the first observations of molecular alignment by several decades [16]. Furthermore, coherent superposition of rotational eigenstates has extensively been exploited in the determination of molecular structures using rotational recurrence spectroscopy [17–19]. These experiments have relied on different types of indirect detection, such as degenerate four-wave mixing, electron diffraction [20], Raman induced polarization spectroscopy [21–24] and high harmonic generation. A more direct observation of alignment is possible using time-resolved imaging of ionic products that are obtained by dissociative ionization or Coulomb explosion. When performed using lasers in the visible/near-infrared part of the spectrum, these measurements require strong laser fields, since many photons are needed in order to induce dissociative/multiple ionization. As a result, the strong laser field that is used to determine the molecular alignment itself influences the angular distribution of the molecular sample. Methods to circumvent this problem have been the use of a probe laser polarization perpendicular to the polarization axis of the alignment (pump) laser beam [6] and the use of circularly polarized probe laser beams [25]. However, in the latter case the ionization probability is still higher in the plane of polarization which can affect the observation of the alignment, especially when molecules are periodically aligned perpendicularly to the polarization of the light (planar delocalization). An alternative method was introduced by Stapelfeldt and co-workers [26], who dissociated aligned molecules by means of a 1-photon process with a short femtosecond laser pulse and subsequently ionized neutral fragments using resonance-enhanced multi-photon ionization (REMPI). In all these imaging probes, parent molecular alignment can be measured providing that the dissociation process is significantly faster than the rotation of the molecule, and that the fragments have a narrow recoil distribution in the molecular frame (axial recoil approximation). These requirements are not necessarily fulfilled, since the evolution on the dissociative potential energy surface is not necessarily fast. Moreover, the final angular distribution measured on the detector is a convolution between dissociation

probability (involving *a priori* parallel and perpendicular transitions) and real spatial alignment.

In the present paper we have applied high harmonics resulting from the interaction of an intense femtosecond laser with an atomic medium to dissociatively ionize molecules that have undergone dynamic alignment as a result of the interaction with an intense near-infrared femtosecond laser pulse. High harmonic generation is a technique that allows the production of short pulses in the extreme ultra-violet (XUV) part of the spectrum with a duration that ranges from the picosecond to the attosecond domain [27, 28]. High harmonic pulses may be used to investigate both nuclear [29, 30] and electronic motions [31]. Here we present the first experimental results using short XUV pulses as a probe of field-free alignment revival structures. This is achieved by using a pump-probe IR/XUV arrangement combined with ion velocity map imaging detection. Ion fragment kinetic energy and angular distributions resulting from dissociative ionization and/or Coulomb explosion of dynamically aligned  $\text{N}_2$  and  $\text{CO}_2$  molecules are reported. These experiments pave the way for future work applying XUV/soft X-ray photoionization and angle-resolved photoelectron spectroscopy to dynamically aligned molecules, which at low photoelectron kinetic energies can provide insight into the electronic structure of molecules and which at high photoelectron kinetic energies can lead to a determination of the molecular structure as a result of electron diffraction in the molecular frame.

## 2. Experimental setup

In the experiment (figure 1) the output of a 1 kHz femtosecond laser (40 fs, 1.8 mJ) is split into two arms. After passing through a delay stage, the pump IR beam is used to create a rotational wavepacket by impulsive stimulated Raman scattering.

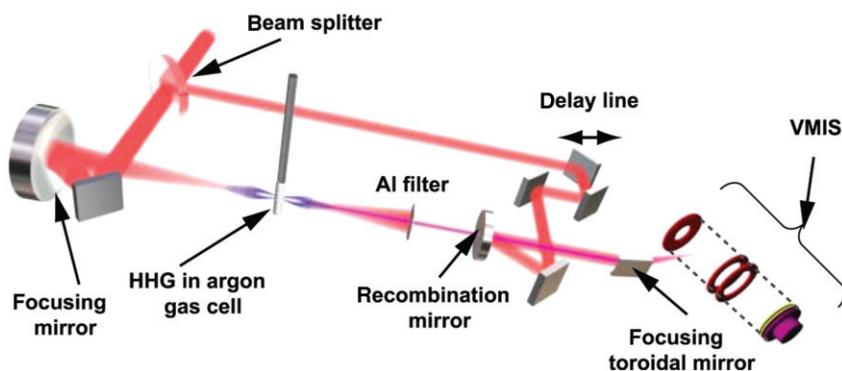


Figure 1. The experimental set-up combines an IR pump/XUV probe arrangement with a velocity map imaging detector. Short XUV pulses are produced via harmonic generation in an argon gas cell and are focused into the experiment co-linearly with an IR beam that is delayed with respect to the XUV beam by means of a delay line in the pump laser beam path. (The colour version of this figure is included in the online version of the journal.)

The second IR beam is used for the generation of high harmonics and the synthesis of short XUV pulses. The harmonics are generated in an argon cell held at a static pressure of 20 mbar. Low-order harmonics are removed by means of an aluminium filter. The resulting XUV beam has a duration of 30 fs and consists of odd harmonics from the 13th up to the 35th order, corresponding to a photon energy in the range between 20 to 55 eV. The pump IR and probe XUV beam are recombined using a concave spherical mirror and focused onto the molecular beam using a toroidal platinum mirror. The molecular beam is produced using a piezoelectric pulsed valve and crosses the light beams on the symmetry axis of a velocity map imaging spectrometer. A static electric field in the spectrometer accelerates ions or electrons formed at the crossing point of the laser and the molecular beam to a position-sensitive detector consisting of a set of micro-channel plates followed by a phosphor screen and a CCD camera. Particle impacts are recorded via a binning routine. Different ionic species are selectively measured by time-gating the voltages applied on the detector. The 3D velocity distribution is reconstructed from the measured 2D projection using a mathematical inversion procedure [32]. IR pump/XUV probe measurements were performed for  $\text{N}_2$  and  $\text{CO}_2$  molecules, varying the delay between the two beams over a range of several picoseconds. In doing so, the IR intensity was kept at a low enough level to avoid any ionization or dissociation from the pump alone. Assuming that molecules stay in their electronic and vibrational ground state, the effect of the IR excitation is to prepare a rotational wave packet via Raman transitions, thereby giving rise to rotational revivals at time delays that are determined by the rotational constant of the molecule.

### 3. Results: IR pump-XUV probe spectroscopy of $\text{N}_2$

A typical two-dimensional image resulting from the detection of  $\text{N}^+$  ions produced in the dissociative ionization of  $\text{N}_2$  is shown in figure 2(a). The corresponding kinetic energy spectrum is shown in figure 2(b). Three distinct contributions are observed, namely a very low energy part (corresponding to the intensity in the very centre of the image), a contribution that peaks around 1.5 eV and a broad, high energy part that has its maximum around 5 eV. The first contribution corresponds to ions that have not acquired any recoil energy and is attributed to the detection of stable doubly-charged molecules  $\text{N}_2^{2+}$ . The  $\sim 1.5$  eV kinetic energy contribution is attributed to excitation processes resulting in dissociative ionization ( $\text{N}_2 \rightarrow \text{N} + \text{N}^+$ ). Fragments resulting from this mechanism display the characteristics of a parallel transition. If the  $\text{N}_2$  molecule is doubly ionized, Coulomb explosion results in the production of two  $\text{N}^+$  ions:  $\text{N}_2^{2+} \rightarrow \text{N}^+ + \text{N}^+$ . Again, the angular distribution is peaked along the laser polarization axis and the kinetic energy range is centred on 5 eV. Samson and Angel [33] have performed a time-of-flight experiment with synchrotron radiation from the dissociative ionization threshold to 107 eV and have reported ion kinetic energy spectra that are very similar to the ones obtained in our experiment. The kinetic energy distributions show two main structures peaked around 1 and 4 eV. The first dissociative ionization threshold of the  $\text{N}_2$  molecule is quite high (at 24.29 eV with respect to the ground state) and results in the production

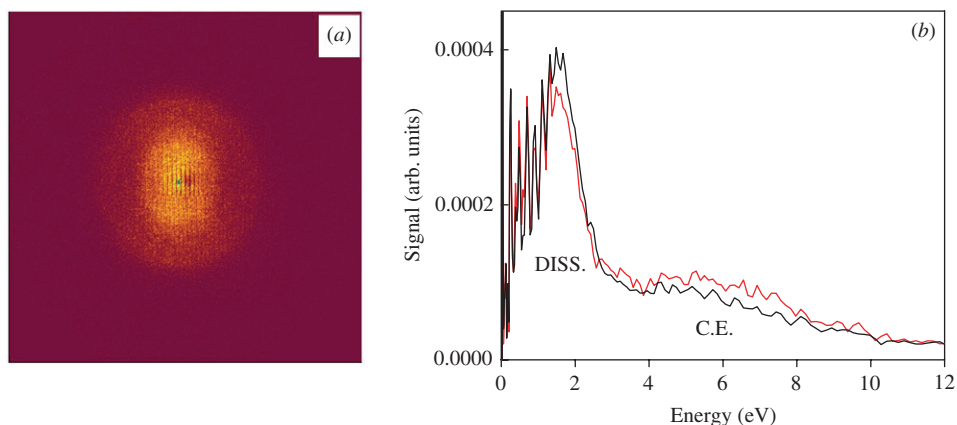


Figure 2. (a) Typical image obtained for the detection of  $N^+$  ions in IR pump/XUV probe experiments on  $N_2$ . Two main contributions are observed that are assigned to dissociative ionization and Coulomb explosion, respectively; (b) the corresponding kinetic energy spectrum, containing a structured contribution from the dissociative ionization channel (DISS.) (0...3 eV) and a contribution from the Coulomb explosion channel (C.E.) (up to 10 eV). The thick black curve was measured for an IR–XUV delay of 5 ps. At zero delay (thin red line), the Coulomb channel explosion is enhanced and extends to higher energy. This is explained by the population of higher excited states in two-colour transitions (see text). (The colour version of this figure is included in the online version of the journal.)

of  $N^+(^3P)+N(^4S)$ . It is followed by additional ionization thresholds leading to the production of  $N^+(1D)+N(^4S)$  (26.19 eV) and  $N^+(^3P)+N(^2D)$  (26.68 eV). Recent work by Nicolas *et al.* [34] has discussed the assignment of excited states responsible for the dissociation process in the range of 24–32 eV using threshold photoelectron–photoion coincidence (TPEPICO) techniques. In that energy range at least five electronic excited states can contribute to the spectrum, however the vibrational progression observed in the photoelectron spectrum suggests that the  $C^2\Sigma_u^+$  state (between vibrational states  $\nu=3$  and  $\nu=11$ ) gives the main contribution. The  $C^2\Sigma_u^+$  state is predissociative and dissociation through the  $B^2\Sigma_u^+$  state via spin–orbit coupling has been proposed as the main decay mechanism. For excitation above  $\nu=12$  of the  $C^2\Sigma_u^+$  state the second dissociative ionization threshold is reached and coupling to the  $d^4\Sigma_u^+$  state is proposed. As soon as the third dissociative ionization channel ( $N^+(^3P)+N(^2D)$ ) opens up (at 26.68 eV), direct dissociation leading to the production of an  $N^+(^3P)$  ground state nitrogen ion becomes the main channel. Nevertheless, above 25 eV many other electronic states can contribute to the spectrum and the high density of electronic states prevents any definitive assignment. In the present experiment, the photon energy range available covers all three dissociative ionization thresholds mentioned. Between 0 and 2 eV the kinetic energy spectrum is highly structured. The peaks observed are consistent with a vibrational progression of the  $C^2\Sigma_u^+(N_2^+)$  state, however above 1 eV (which corresponds to  $\nu=11$ ) the spectrum is more complicated and the finite resolution of our spectrometer does not allow one to resolve and assign any states. A broad structure

is observed for the dissociation channel between 1.5 and 3 eV which corresponds to contributions of many electronic states.

The first threshold for the dissociation of  $N_2^{2+}$  is at 38.8 eV and allows the separation of the molecule in  $N^+(^3P)+N^+(^3P)$  fragments. Besnard *et al.* [35] have studied fragmentation processes of  $N_2^{2+}$  induced by synchrotron radiation in the range of 45–60 eV using photoion–photoion coincidence (PIPICO). They showed that six electronic excited states of the dication can be involved in the production of two  $N^+$  ions. The kinetic energy release was measured and assigned to the relevant states. The  $^1\Pi_u$ ,  $^3\Sigma_g^-$ ,  $^1\Delta_g$ ,  $^1\Sigma_g^+$ ,  $^1\Pi_g$ ,  $^3\Delta_u$  states were respectively attributed to ion kinetic energies of 3.2, 3.6, 4.0, 4.5, 5.4 and 7.1 eV. All these states asymptotically converge to the  $N^+(^3P)+N^+(^3P)$  limit. Baldit *et al.* [36] have studied Coulomb explosion of  $N_2$  using a femtosecond laser. Measured  $N^+$  kinetic energy distributions show two main peaks at 4 and 5 eV which have been assigned to the  $^1\Delta_g$  and  $^1\Pi_g$  states. In our experimental results, the kinetic energy spectrum above 3 eV seems to correspond very well with the results obtained with synchrotron radiation and the first five electronic states can be involved. In fact, thresholds for these states were determined between 45.2 and 49.6 eV which correspond to the energy range accessible in our experiment. In our experiments, at zero delay between the IR and XUV pulses, the kinetic energy spectrum is enhanced and extends to a higher energy (see figure 2(b)). A peak is observed around 7 eV which seems to correspond to the  $^3\Delta_u$  state. We postulate that the higher threshold for this state (53 eV) can only be reached in our experiment in a two-colour process involving both the IR and XUV beams. We note that 53 eV corresponds to the energy of the 35th harmonic, which is relatively weak in the experiment.

At non-zero delays, the kinetic energy spectra are consistently similar to the one presented in figure 2(b). Important time delay-dependent changes are observed, however, in the angular distributions of the  $N^+$  fragments produced. These changes reflect the evolving ground state molecular alignment that results from the interaction of the molecules with the intense IR pump laser pulse. In order to characterize this alignment, the expectation value  $\langle \cos^2(\theta) \rangle$  was extracted from each recorded image for both the dissociative ionization and the Coulomb explosion channel. Typical results are shown in figure 3. Both channels clearly show variations of the ion angular distribution corresponding to a half (4.2 ps,  $\Delta T = 1/(4Bc)$ ) and quarter (2.1 ps,  $\Delta T = 1/(8Bc)$ ) revival. In  $N_2$ , both odd and even  $J$  states are populated in the ground vibrational state. However, due to nuclear spin statistics the weight of the population of the even states is two times higher than the one for odd states. As a consequence, the quarter revival observed at 2.1 ps is weaker than the half revival at 4.2 ps. After the maximum alignment, at a delay of approximately 4.5 ps, the molecular sample undergoes a planar delocalization where the axis of the molecule localizes in a plane perpendicular to the light polarization. The revival structure observed is remarkably broad which indicates that the molecular sample was at very low temperature (i.e. only a few initial rotational states are populated). At higher temperatures, many initial rotational states contribute, leading to sharper revival structures [37].

One interest in controlling the rotational degrees of freedom of a molecule comes from the fact that interactions between light and molecules strongly depend on the

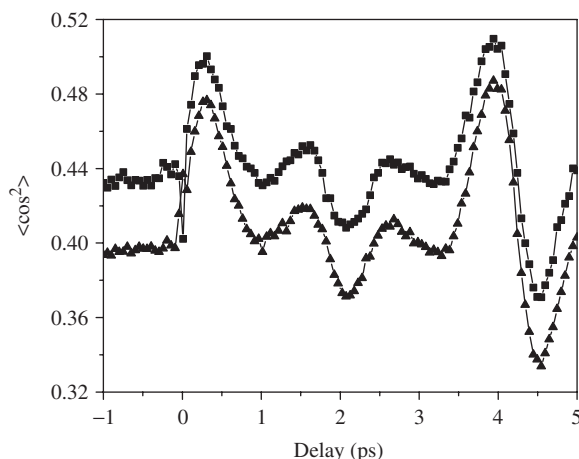


Figure 3. Experimentally observed alignment of  $N^+$  fragments in IR pump/XUV probe experiments on  $N_2$ . The evolution of  $\langle \cos^2(\theta) \rangle$  as a function of the time delay between the IR pump and the XUV probe pulses is shown for the dissociative ionization channel (0...3 eV) (squares) and the Coulomb explosion channel (3 to 10 eV) (triangles). For delays  $<0$  the XUV probe pulse precedes the IR pump pulse and a time-independent anisotropy is measured that reflects the anisotropy of the dissociation, resp. Coulomb explosion process. For delays  $>0$ , both channels show alignment and planar delocalization at quarter and half rotational revivals which occur at delays given by the rotational constant of the molecule.

angle between the molecular axis and the light polarization axis. Light absorption increases when the laser polarization is parallel to the direction of the transition dipole moment. As an illustration of this principle, a measurement of the ion yield versus molecular alignment has been performed. As shown in figure 4, the yield of both the dissociation and Coulomb explosion channels follows the rotational revival structure that was previously observed via the angular distribution. At zero delay, one can observe a depletion of the yield in the dissociative ionization channel and an increase of the yield in the Coulomb explosion channel that is related to a two-colour IR/XUV process increasing the probability for the double ionization process. At later delays, both single ionization (giving rise to the dissociative ionization channel) and double ionization (giving rise to the Coulomb explosion channel) are increased when the molecule is aligned along the light polarization. Hence, both the single photon single and double ionization yields contain the signature of the molecular alignment.

#### 4. Results: IR pump-XUV probe spectroscopy of $CO_2$

Similar results have been obtained for  $CO_2$  molecules, where dissociative ionization and Coulomb explosion following the absorption of XUV radiation can produce  $O^+$ ,  $C^+$  and  $CO^+$  fragments. In the following discussion we will focus on the  $O^+$  ion signal. A typical image and kinetic energy spectrum measured is presented in figure 5. Similarly as for the case of  $N_2$ , one can clearly distinguish two main contributions

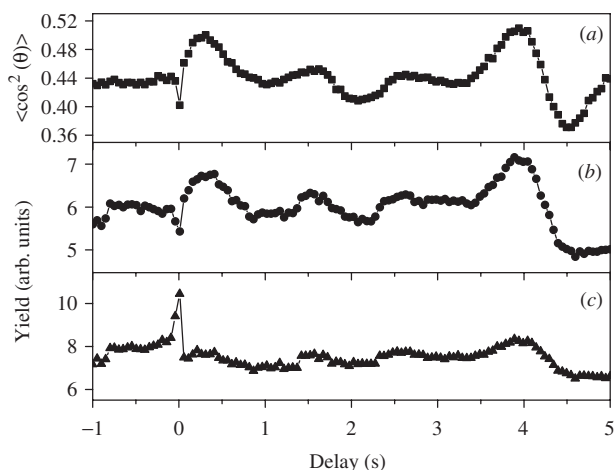


Figure 4.  $\text{N}^+$  ion yields in IR–XUV probe experiments on  $\text{N}_2$ , measured as a function of pump–probe time delay. The time-dependent molecular alignment  $\langle \cos^2(\theta) \rangle$  (a) is compared to the variations of the ion yield in the dissociative ionization channel (b) and to the Coulomb explosion channel (c). The yield strongly depends on the time delay, and shows a similar structure as the time-dependence alignment.

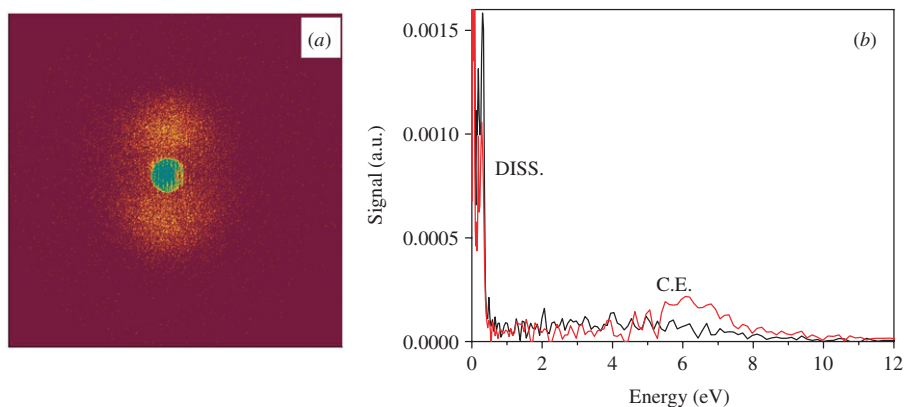


Figure 5. (a) Typical image obtained for the detection of  $\text{O}^+$  ions in experiments on  $\text{CO}_2$ . Two main contributions are observed resulting from dissociative ionization and Coulomb explosion; (b) corresponding kinetic energy spectrum showing the dissociative channel (DISS.) (0.5 eV) and the Coulomb explosion channel (C.E.) (up to 10 eV) (thick black line). The solid curve was measured for an IR–XUV delay of 10 ps. At zero delay a shift of the kinetic energy distribution for the Coulomb explosion channel is observed (thin red line), which corresponds to the opening of the atomization channel (see text). (The colour version of this figure is included in the online version of the journal.)

related to dissociative ionization (below 0.5 eV) and Coulomb explosion (around 5 eV). The resolution of the spectrometer does not allow us to resolve any structure in the dissociative ionization channel but the maximum energy observed agrees with previous studies of photodissociation [38] of  $\text{CO}_2^+$  where  $\text{O}^+$  is produced in the  $^4\text{S}_u$  state from the  $\text{C}^2\Sigma_g^+$  state of  $\text{CO}_2^+$ .

In the Coulomb explosion channel, the kinetic energy release of  $\text{CO}_2^{2+}$  has been studied by Masuoka *et al.* [39] using PIPICO and synchrotron radiation in the range from 40 to 100 eV. Between 40 and 50 eV, the total kinetic energy release (KER) produced in the  $\text{CO}^+ + \text{O}^+$  process slowly increases when the photon energy increases. The average KER varies from 4 eV at threshold to 5.5 eV at 50 eV and involves several decay channels:  $\text{CO}^+(\text{X}^2\Sigma_g^+) + \text{O}^+(\text{P}_u)$ ,  $\text{CO}^+(\text{X}^2\Sigma_g^+) + \text{O}^+(\text{D}_u)$ ,  $\text{CO}^+(\text{A}^2\Pi_u) + \text{O}^+(\text{S}_u)$ ,  $\text{CO}^+(\text{X}^2\Sigma_g^+) + \text{O}^+(\text{S}_u)$ . Above 50 eV, the kinetic energy of the  $\text{O}^+$  ion coming from the  $\text{CO}^+ + \text{O}^+$  channel stays constant. This is due to the opening of a new dissociative channel. As discussed by Masuoka *et al.*, the excited states populated above 50 eV follow a slightly more complicated path giving rise to the complete atomization of the molecule into  $\text{C}^+ + \text{O}^+ + \text{O}$ . The KER measured for the  $\text{CO}^+ + \text{O}^+$  channel seems to correspond very well to our measurements in which the complete energy range (40 to 50 eV) is covered. At zero delay the kinetic energy spectrum is shifted by 1 eV (figure 5(b)). We postulate that this corresponds to the opening of the atomization channel where  $\text{C}^+ + \text{O}^+ + \text{O}$  is produced, which is possible for a total energy higher than 50 eV and hence requires the presence of both laser beams. In the PIPICO experiment, the KER for the atomization channel increases with the photon energy. The average KER is 8 eV for a photon energy of 60 eV which agrees with our measurements. The average KER in the atomization channel is higher than in the Coulomb explosion channel, since the internuclear distances that lead to the formation of  $\text{C}^+ + \text{O}^+ + \text{O}$  are smaller than the ones that lead to  $\text{CO}^+ + \text{O}^+$ . For non-zero time delays, the  $\text{O}^+$  KER spectrum stays constant and reveals a main contribution due to the  $\text{CO}^+ + \text{O}^+$  channel. A kinetic energy of 4.8 eV was previously measured in a strong field ionization experiment using 40 fs near-infrared (Ti:sapphire) laser pulses [40], and is comparable to the KER that we have obtained in the present case.

The evolution of the angular distributions of the  $\text{O}^+$  kinetic energy spectrum is presented in figure 6. Due to the symmetry of the  $\text{CO}_2$  molecule only even  $J$  states are populated in the ground vibrational state, and the revivals that are observed correspond respectively to the quarter (10.6 ps) and the half (21.2 ps) revival. Surprisingly, the dissociation channel exhibits no angular variation whereas the Coulomb explosion channel shows very pronounced revivals. This suggests that the dissociative ionization involves long-lived intermediate states, allowing for significant rotation of the molecule between the instant of excitation and the time of dissociation.

The ionic yield in the  $\text{O}^+ + \text{CO}$  and the  $\text{O}^+ + \text{CO}^+$  channels as a function of pump-probe delay is shown in figure 7. For both channels a very pronounced dependence is observed. The fact that the dependence of the ionic yield on time delay is visible both in the Coulomb explosion and the dissociative ionization channel whereas no time-dependent alignment was observed in the dissociative ionization channel again points out the role of excited state lifetimes in the dissociative ionization. Clearly, both single and double ionization are more probable when the molecule is aligned with the light polarization. In  $\text{CO}_2$  the influence of molecular alignment appears to be stronger than in  $\text{N}_2$ . This can be attributed to the higher anisotropic polarizability of the molecule which gives a more efficient coupling with the IR field and hence an enhanced alignment.

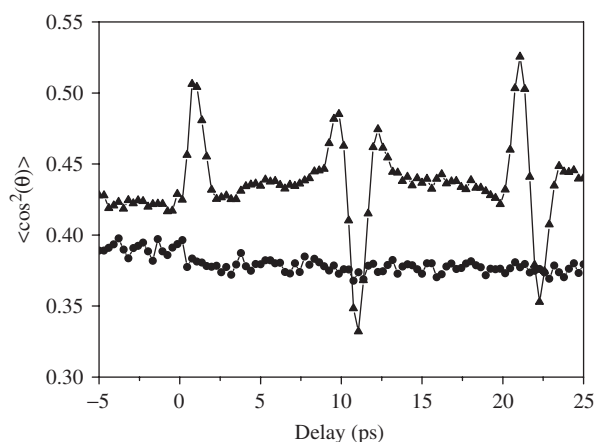


Figure 6. Experimentally observed alignment of  $\text{O}^+$  fragments in experiments on  $\text{CO}_2$ . The evolution of  $\langle \cos^2(\theta) \rangle$  as a function of the time delay between the IR pump and XUV probe pulses is shown, as measured for the dissociative ionization channel (00.5 eV) (circles) and the Coulomb explosion channel (0.5 to 10 eV) (triangles). For delays  $< 0$  the XUV probe pulse precedes the IR pump pulse and a time-independent anisotropy is measured that reflects the anisotropy of the dissociation, resp. Coulomb explosion process. For delays  $> 0$ , the Coulomb explosion channel shows alignment and planar delocalization at quarter and half rotational revivals which occur at delays given by the rotational constant of the molecule. The dissociative ionization channel does not show a time-dependent anisotropy, which may be due to the lifetime of the excited state.

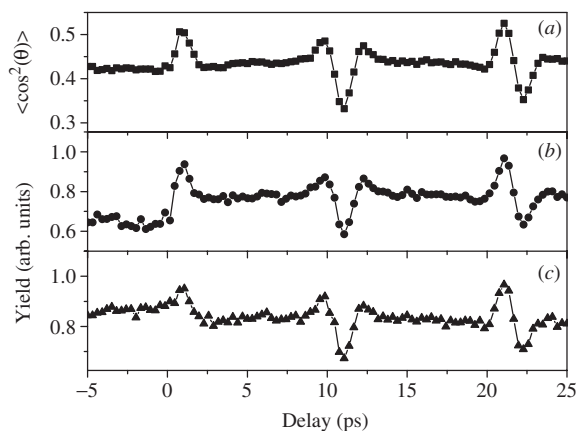


Figure 7. Comparison of the molecular alignment  $\langle \cos^2(\theta) \rangle$  in the Coulomb explosion channel (a) to the evolution of the  $\text{O}^+$  ion yield for the dissociative ionization and the Coulomb explosion channel with pump-probe time delay in IR-XUV pump-probe experiments on  $\text{CO}_2$ . The ion yields in the dissociative ionization channel (b) and the Coulomb explosion channel (c) strongly depend on time delay, and show a similar structure as the time dependence of the angular distribution. The yields of both single and double ionization reflect the angular distribution and are as a signature of the alignment of the molecule. Near-zero time delay the ion yield in the Coulomb explosion channel shows an enhancement, whereas the yield in the dissociative ionization channel drops, due to a two-colour IR-XUV process that enhances the former at the expense of the latter.

## 5. Discussion and outlook

In the previous section we have discussed how field-free molecular alignment is observed by means of ionization with an XUV photon that induces a dissociative ionization and/or Coulomb explosion. We showed that the ionization yield can also be used as a signature of the molecular axis alignment along the light polarization. When the molecular alignment is at a maximum, the axes of the molecules are fixed in space. If the angularly resolved photoelectron kinetic energy spectrum evolution is measured over a rotational revival, information on the molecular frame photoelectron spectrum can be obtained. So far, molecular frame photoelectron measurements have been recorded via coincidence techniques which require dissociative ionization of the molecule in order to recover the molecular frame information from laboratory frame measurements [41]. In the present technique the axis of the molecule is fixed in space and dissociation of the molecule is not, *a priori*, necessary. As a consequence even threshold ionization can be studied. Generally photoelectron spectroscopy in the molecular frame would provide information on the electronic structure of the molecule from threshold to high energy states. We performed a first attempt on  $N_2$  where angularly resolved electron spectra were recorded at different delays over a rotational revival. As shown in figure 8 no clear evidence for a variation of the angular distribution with respect to the alignment of the molecule was observed. Tsubouchi and Suzuki [42] have simulated the photoelectron angular distribution obtained in 1-photon and 2-photon REMPI of the sigma orbital of  $N_2$  molecules that were dynamically aligned with an intense femtosecond laser pulse. The evolution

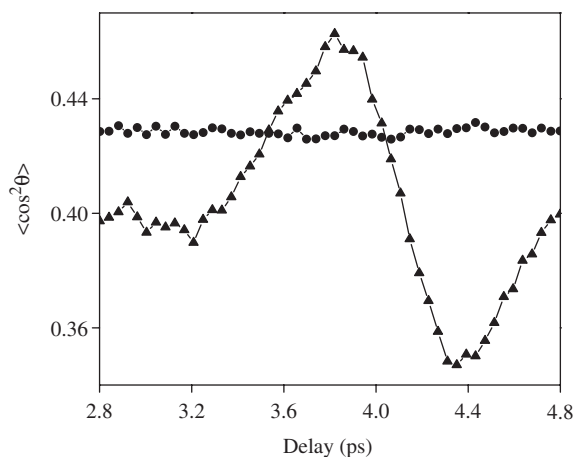


Figure 8. Evolution of  $\langle \cos^2(\theta) \rangle$  for the detection of  $N^+$  ions resulting from the dissociative ionization of  $N_2$  (triangles) along with the evolution of  $\langle \cos^2(\theta) \rangle$  for the photoelectrons that accompany this process (circles), both given as a function of the time delay between IR pump and XUV probe. The measurement is performed in the vicinity of the quarter rotational revival where the  $N^+$  measurements show a pronounced time-dependent alignment. However, no time dependence is observed in the photoelectron angular distributions, which can be explained by the symmetry of the molecular orbitals.

of the angular distribution calculated over the full rotational revival at 8.2 ps varies only weakly and they conclude that laboratory frame and molecular frame angular distributions are quite similar in that case. The variation is actually very small and may not be easily observed in the present experimental results. This could simply be explained by the fact that the orbital from which electrons are removed is isotropic which makes  $N_2$  a bad candidate for such experiments.

Another very intriguing and promising aspect of angularly resolved electron kinetic energy spectra concerns the effect of the molecular structure on the continuum electronic wavefunction. Generally, the photoelectron angular distribution contains information on the phases of the different electronic partial waves involved in a photoionization process. When the De Broglie wavelength of electrons emitted by the atoms of a molecule is comparable to the internuclear distance in the molecule interference effects can be observed. For electrons the relation between the kinetic energy  $\varepsilon$  and the corresponding De Broglie wavelength  $\lambda$  is given by  $\varepsilon[\text{eV}] = 150/\lambda[\text{\AA}]^2$ .

In a recent experiment Sanov and co-workers [43] have studied the dissociation of  $I_2^-$  using a pump-probe arrangement coupled with a photoelectron imaging spectrometer. An oscillation of the asymmetry parameter characterizing the photoelectron angular distribution was observed over a 2.5 ps delay. The explanation proposed by the authors relies on the interference between the electronic waves emitted by the two atoms when the electron wavefunction is delocalized on the two atoms. In this experiment the interference effect comes mainly from the phase difference accumulated by the photoelectron along the distance between the two nuclei. Effects of the nuclei themselves are considered as an additional phase and would explain the slight discrepancy between the experimental results and the simple two-centre interferometer model proposed. When electron kinetic energies reach approximately 100 eV, as they easily can in experiments with harmonics, molecular structure can be probed via diffraction effects. Moreover, rotational revivals offer a time window atomic dynamics and its impact on molecular structure can be studied [44–47].

In the Sanov experiment the oscillation of the angular distribution fades out when the electron gets localized on one specific atom which allows testing inversion symmetry in  $I_2^-$ . More generally electron localization in molecules takes place over timescales that range from picoseconds to attoseconds [48, 49]. The Raman process responsible for the field-free alignment is *itself* an example of the effect of the electron localization, as dynamic alignment is a consequence of the laser-induced dipole moment. Field-free molecular alignment was discussed in the present paper but the fundamental process that allows the creation of such rotational wavepackets has not been directly observed so far due to the extremely fast time scale at which the process occurs [50]. In a Raman process, the electronic wavefunction of the molecule transiently becomes a superposition of the ground state and one or more electronically excited virtual states. The interaction of the polarizability with the electric field of the laser forces the molecule to gain or lose rotational quanta. In other words, the nuclear motion is a direct consequence of the electronic dynamics. During the interaction between the IR field and the molecule, the electron localization in the molecule follows the electric field of the laser [51]. Over one optical cycle, the electron cloud oscillates and, in a diatomic molecule, is successively located on one or the

other atom. If one can dissociate the molecule using an attosecond pulse, then the angularly resolved ion kinetic energy spectrum might reveal oscillations in the dissociative ionization channel along the direction of the polarization of the light. This might reveal a localization of the electrons mainly on one of the two atoms of the molecule. The ion produced would correspond to the atom where the electrons are not localized anymore. In such an experiment one attosecond pulse per IR cycle is required in order not to cancel the 'up/down' asymmetry.

In conclusion, short XUV pulses have been shown to be a clean probe of field-free molecular alignment. The kinetic energy spectra obtained are quite similar to the ones obtained in the strong field regime. The one-photon nature of the process allows us to avoid the question of the influence of the laser electric field of the probe on the molecular alignment. The single and double ionization yields have been shown to be a clear signature of the molecular alignment. These results will give the opportunity to perform molecular frame experiments including electronic threshold spectroscopy and electron diffraction measurements. It also paves the way to study attosecond electronic dynamics in molecules.

### Acknowledgements

We are grateful to J. Mauritsson for his work on figure 1. We acknowledge support by the Marie Curie Research Training Networks XTRA (MRTN-CT-2003-505138) and PICNIC (HPRN-2002-00183) and by a Marie Curie Intra-European Fellowship, (MEIF-CT-2003-500947, MFK). The research of FL, MFK, JIK, YN, OG, TM and MJJV is part of the research programme of the 'Stichting voor Fundamenteel Onderzoek der Materie (FOM)', which is financially supported by the 'Nederlandse Organisatie voor Wetenschappelijk Onderzoek (NWO)'. KV is on leave from the Department of Optics and Quantum Electronics, University of Szeged, Hungary. The present address of FL is Laboratoire de Spectrométrie Ionique et Moléculaire, Université Claude Bernard Lyon 1 & CNRS, France. This research was supported by a Marie Curie Intra-European Fellowship (MEIF-CT-2004-009268, KV), the Marie Curie Research Training Network XTRA (MRTN-CT-2003-505138), the Integrated Initiative of Infrastructure LASERLAB-EUROPE (RII3-CT-2003-506350) within the 6th European Community Framework Programme, the Knut and Alice Wallenberg Foundation and the Swedish Science Council.

### References

- [1] J. Posthumus, Rep. Prog. Phys. **67** 623 (2004).
- [2] P.B. Corkum, C. Ellert, M. Mehendale, *et al.*, Faraday Discuss. Roy. Soc. Chem. **113** 47 (1999).
- [3] J.J. Larsen, H. Sakai, C.P. Safvan, *et al.*, J. Chem. Phys. **111** 7774 (1999).
- [4] M.J.J. Vrakking and S. Stolte, Chem. Phys. Lett. **271** 209 (1997).
- [5] T. Seideman, Phys. Rev. Lett. **83** 4971 (1999).
- [6] F. Rosca-Pruna and M.J.J. Vrakking, Phys. Rev. Lett. **87** 153902 (2001).
- [7] A.T.J.B. Eppink and D.H. Parker, Rev. Sci. Instrum. **68** 3477 (1997).

- [8] C.Z. Bisgaard, M.D. Poulsen, E. Péronne, *et al.*, Phys. Rev. Lett. **92** 173004 (2004).
- [9] J.J. Larsen, K. Hald, N. Bjerre, *et al.*, Phys. Rev. Lett. **85** 2470 (2000).
- [10] R.A. Bartels, T.C. Weinacht, N. Wagner, *et al.*, Phys. Rev. Lett. **88** 013903 (2002).
- [11] R. Velotta, N. Hay, M.B. Mason, *et al.*, Phys. Rev. Lett. **87** 183901 (2001).
- [12] S.C. Althorpe and T. Seideman, J. Chem. Phys. **110** 147 (1999).
- [13] Y. Arasaki, K. Takatsuka, K. Wang, *et al.*, J. Chem. Phys. **114** 7941 (2001).
- [14] J. Itatani, J. Levesque, D. Zeidler, *et al.*, Nature **432** 867 (2004).
- [15] T. Kanai, S. Minemoto and H. Sakai, Nature **435** 470 (2005).
- [16] J.P. Heritage, T.K. Gustafson and C.H. Lin, Phys. Rev. Lett. **34** 1299 (1976).
- [17] J.S. Baskin, P.M. Felker and A.H. Zewail, J. Chem. Phys. **84** 4708 (1986).
- [18] P.M. Felker and A.H. Zewail, J. Chem. Phys. **86** 2460 (1987).
- [19] J.S. Baskin, P.M. Felker and A.H. Zewail, J. Chem. Phys. **86** 2483 (1987).
- [20] K. Hoshina, K. Yamanouchi, T. Ohshima, *et al.*, Chem. Phys. Lett. **353** 27 (2002); K. Hoshina, K. Yamanouchi, T. Ohshima, *et al.*, Chem. Phys. Lett. **353** 33 (2002).
- [21] E. Hertz, O. Faucher, B. Lavorel, *et al.*, Phys. Rev. A **61** 033816 (2000).
- [22] Y. Chen, L. Hunziker, P. Ludowise, *et al.*, J. Chem. Phys. **97** 2149 (1992).
- [23] V. Renard, M. Renard, S. Guérin, *et al.*, Phys. Rev. Lett. **90** 153601 (2003).
- [24] S. Zamith, Z. Ansari, F. Lépine, *et al.*, Opt. Lett. **30** 2326 (2005).
- [25] Ch. Ellert and P.B. Corkum, Phys. Rev. A **59** R3170 (1999).
- [26] E. Péronne, M.D. Poulsen, C.Z. Bisgaard, *et al.*, Phys. Rev. Lett. **91** 043003 (2003).
- [27] A. L'Huillier and Ph. Balcou, Phys. Rev. Lett. **70** 774 (1993).
- [28] P.M. Paul, E.S. Toma, P. Breger, *et al.*, Science **292** 1689 (2001).
- [29] V. Chikan, B. Nizamov and S.R. Leone, J. Phys. Chem. A **110** 2850 (2006).
- [30] S.L. Sorensen, O. Bjørneholm, I. Hjelte, *et al.*, J. Chem. Phys. **112** 8038 (2000).
- [31] R. Kienberger, M. Hentschel, M. Uiberacker, *et al.*, Science **297** 114 (2002).
- [32] M.J.J. Vrakking, Rev. Sci. Instrum. **72** 4084 (2001).
- [33] J.A.R. Samson and G.C. Angel, Phys. Rev. A **42** 1307 (1990).
- [34] C. Nicolas, C. Alcaraz, R. Thissen, *et al.*, J. Phys. B **36** 2239 (2003).
- [35] M.J. Besnard, L. Hellner, G. Dujardin, *et al.*, J. Chem. Phys. **88** 1732 (1988).
- [36] E. Baldit, S. Saugout and C. Cornaggia, Phys. Rev. A **71** 021403 (2005).
- [37] H. Stapelfeldt and T. Seideman, Rev. Mod. Phys. **75** 543 (2003).
- [38] J. Liu, W. Chen, M. Hochlaf, *et al.*, J. Chem. Phys. **118** 149 (2003).
- [39] T. Masuoka, E. Nakamura and A. Hiraya, J. Chem. Phys. **104** 6200 (1996).
- [40] Ph. Hering and C. Cornaggia, Phys. Rev. A **59** 2836 (1999).
- [41] M. Lebech, J.C. Houver, A. Lafosse, *et al.*, J. Chem. Phys. **118** 9653 (2003).
- [42] M. Tsubouchi and T. Suzuki, Phys. Rev. A **72** 022512 (2005).
- [43] R. Mabbs, K. Pichugin and A. Sanov, J. Chem. Phys. **123** 054329 (2005).
- [44] T. Zuo, A.D. Bandrauk and P.B. Corkum, Chem. Phys. Lett. **259** 313 (1996).
- [45] M. Lein, J. Marangos and P. Knight, Phys. Rev. A **66** 051404 (2002).
- [46] H. Niikura, F. Legare, R. Hasbani, *et al.*, Nature **417** 917 (2002).
- [47] M. Spanner, O. Smirnova, P.B. Corkum, *et al.*, J. Phys. B: At. Mol. Opt. Phys. **37** L243 (2004).
- [48] M.F. Kling, Ch. Siedschlag, A.J. Verhoef, *et al.*, Science **312** 246 (2006).
- [49] S. Chelkowski, G.L. Yudin and A.D. Bandrauk, J. Phys. B: At. Mol. Opt. Phys. **39** S409 (2006).
- [50] M.J.J. Vrakking, Phys. Scr. **73** C36 (2006).
- [51] A.D. Bandrauk, S. Chelkowski and H.S. Nguyen, Int. J. Quantum Chem. **100** 834 (2004).